Bathymetry and Crustal Thickness Variations from Gravity Inversion and Flexural Isostasy

Carla Braitenberg, Elena Pagot
Department of Earth Sciences, Trieste University, Via Weiss 1, 34100 Trieste, Italy
Berg@univ.trieste.it

Yong Wang, Jian Fang
Institute of Geodesy and Geophysics, Chinese Academy of Sciences, 54 Xu Dong Road, 430077 Wuhan, P.R. China

Abstract. The satellite-derived gravity field over the South China Sea is used to obtain a model of crustal thickness variations and of the bathymetry. Constraining data are the crust-mantle interface depth values recovered from seismic studies and the shipborne bathymetry measurements. Essential for the modeling is furthermore the isostatic flexure model, which is numerically evaluated in terms of a convolutional approach, thus overcoming the problems connected to spectral analysis. The flexure model and the gravity model of crustal thickness variations agree very well over all of the basin, except for a near to linear trend present in the gravity data, that could be due to deeper lying sources. The crustal model allows to isolate the gravity contribution of the bathymetry from the total observed field, which can be used to improve the bathymetry. Both gravity anomaly and inverted bathymetry delineate the central basin rift very well, a structure not well recovered from the shiptrack bathymetric sounding.

Keywords. Satellite altimetry, gravity, flexural isostasy, bathymetry, crustal thickness, South China Sea

1 Introduction

The observed gravity field over the earth surface is generated by the 3D density variations in the earth. A full modeling of the observed field requires a density model that assigns variable density in function of depth and position. The full density modeling is feasible only in the case that independent constraining data are available, as the problem does not have a unique solution. An approximation to the crustal model can be achieved by reducing the complexity of the model, and making use of an ubiquitous property of the upper layers of the earth's crust, given by some well defined density jumps. Over oceanic areas the biggest jump is between bathymetry and water, further jumps regard the transition from sediments to oceanic crust, and the jump at the crust-mantle discontinuity. In a simplified crustal model, the gravity field may be explained by the undulations of the surfaces defined by the major discontinuities in density, and viceversa can the depth variations of the discontinuity be inverted from the gravity data. To a certain extent the contributions of the sources set at different depth levels can be separated by wavelength filtering, thus allowing the modeling of the upper or lower discontinuity. The isostatic compensation model gives a physical basis for the relation between the topography/bathymetry or in more general terms the crustal load and the crustal thickness variations. The isostatic compensation concept has been particularly successful in oceanic areas, where the elastic thickness T_e, one of the parameters which controls the flexural response, has been shown to correlate well with the age of crustal loading (Watts, 2001). With a given topography/bathymetry, the long wavelength gravity field is controlled by the elastic thickness value, which determines the variation of the crust-mantle interface (CMI) and consequently the gravity signal produced by the corresponding density discontinuity.

Studies concerned with the recovery of bathymetry from satellite derived gravity data adopt the short wave length gravity signal, and eliminate the long wavelength signal from the inversion process, in order to reduce the effects from the crustal thickness variations. Adopting the remove-restore method (e.g. Smith and Sandwell, 1997; Sandwell and Smith, 2001) the bathymetry in the long-wavelength is that of the starting model, and the inversion is restricted to the short-wavelengths.

International Association of Geodesy Symposia, Vol. 126
C Hwang, CK Shum, JC Li (eds.), International Workshop on Satellite Altimetry

In the present study we aim at an interpretation of the gravity signal in terms of both the crustal thickness variations and the bathymetry in the South China Sea. It is investigated whether the isostatic flexural model is compatible with the proposed crustal model. All available constraints, as shipborne bathymetric depths and seismic evaluation of the depth of the CMI are considered.

For the gravity inversion we follow the iterative method described in Braitenberg et al. (1997). The flexural isostatic calculations are based on the thin plate flexure model, described with many applications in Watts (2001). The calculations of the crustal flexure were made with a convolution approach, described in Braitenberg et al. (2002).

We investigate the crustal thickness variations and bathymetry in the South China Sea.

2 Methodology

The approach we use in the inversion of the crustal structure and of the bathymetry involves a series of consecutive steps, which include (A1) gravity inversion and (A2) the calculation of the flexure of the crust beneath the topographic/ bathymetric load. Starting point of the analysis is a database containing gravity observations, observed ship-track bathymetry, crustal thickness estimates from seismic investigations along profiles or single points and, if available, some informations on the sediment layer thickness, and a startup bathymetry/ topography model as ETOPO5. In the following the steps are described in detail.

Step (A1): The first part of the work aims at modeling the CMI depth variations. If no other constraints are available, a constant density contrast across the interface is assumed. Due to the 1/r dependence of the gravity potential field, the short wavelength variations of the gravity field are filtered out greatly with increasing distance to the mass source (e.g. Zadro, 1986; Blakely, 1995). It follows that only the long-wavelength part of the observed gravity field is generated by the CMI undulations, the short-wavelength part being due to the superficial masses. For the CMI undulations to be inverted from the gravity data, the Bouguer correction must be evaluated. This can be accomplished with a starting topography-bathymetry model. The starting model can be created by interpolation of ocean depth measurements along ship-tracks, whenever these are dense enough, or with a global model as ETOPO5, or else by an integration of both. It is not essential that the bathymetric model be of high spatial resolution, as the short-wavelength part of the Bouguer gravity field is not considered in the further processing, but only the long-wavelength part. The Bouguer field is inverted applying an iterative constrained inverse modeling (Braitenberg et al., 1997). The method has been extensively tested on synthetic models (Braitenberg and Zadro, 1999) and in various geographical areas as Alps (Braitenberg et al., 1997; Zadro and Braitenberg, 1997, Ebbing et al., 2001) and Karakorum (Braitenberg and Drigo, 1997). It requires some starting parameters, that are the reference depth of the density interface (d) and the density contrast across the interface ($\Delta\rho$). Furthermore the cut-off wavelength that limits the wavenumber-range used in the inversion must be set. The CMI-depth estimates from seismic investigations are used as constraints for the choice of the two relevant parameters d and $\Delta\rho$.

Step A2: The next step involves the flexure model, which is an independent means to find the CMI-undulations and allows to check for the consistency of the gravity-deduced CMI-undulations. The modeling of the CMI-undulations in terms of the thin plate flexure model is done by a least squares approximation of the gravity CMI evaluated in step A1 of the procedure. The flexure is calculated by the convolution of the crustal load with the pointload flexure response curves, as described in Braitenberg et al, (2002). A set of flexure response curves is prepared, pertaining to the elastic thicknesses ranging from T_e=0 km to T_e=20 km at a step of 0.5 km. On square windows of sidelength L the difference of the gravity CMI and flexure CMI is calculated. The rms difference between the two undulating surfaces is minimized by varying the elastic thickness Te. The result is a solution of the flexed crust that is in best agreement with the long wavelength component of the gravity field.

Step B: Once the flexure CMI has been obtained, the gravity field generated by it is evaluated. This field is then subtracted from the observed gravity, in order to obtain the residual gravity, which is greatly due to the bathymetry.

Step C: The third step is concerned with the inversion of the residual gravity, which results in the bathymetry. Again the inversion depends on two parameters, which are the reference depth and the density contrast. The reference depth in this case is the sea level and the density contrast is the difference between the densities of sea water and the crustal

reference density. The bathymetry along shiptracks is used as a constraint for the choice of the density contrast adopted in the inversion.

In the procedure we have outlined, some distortion of the inverted bathymetry may be due to the gravity effect of the sediments or density variations in crust and mantle. Up to this point of the procedure, the sediment thickness has not been taken into account. For the South China Sea presently no model of sediment thickness is at our hands, so we may not model the gravity effect directly. Presently we correct for these contributions by reducing the very long-wavelength part of the gravity anomaly with a high-pass filter with 800 km cut-off wavelength.

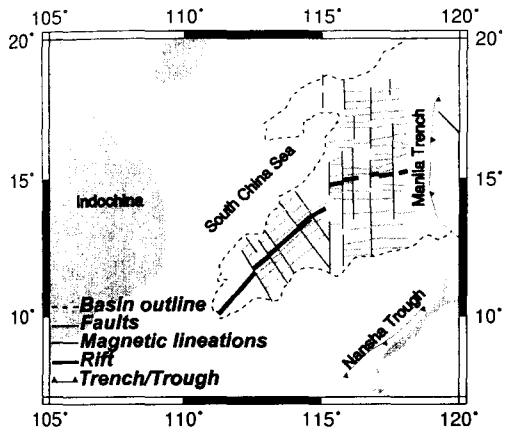

Fig. 1 Tectonic map of the South China Sea, after Map Series of Geology and Geophysics of China Sea and Adjacent Regions (1992).

3 Geological Outline of the South China Sea

The Fig. 1 shows a tectonic map of the South China Sea (after the Map Series of Geology and Geophysics of China Sea and Adjacent Regions, 1992). The ridge running along the center of the basin is shown. The spreading direction and age has been determined from the observations of the magnetic lineations parallel to the ridge. The ridge is divided into the EW-trending northern older segment and the younger SW-NE trending segment. The basin is bounded to the north by the passive South China Sea continental margin, to the West by a postulated transform margin and to the east by the Manila Trench, where oceanic crust is subducted eastward (Nissen et al., 1995). The age of the EW trending magnetic lineations have been estimated to correspond to ages 17-32 Ma, whereas the SW-NE trending lineations are younger and are estimated to be 15.5-24 Ma of age.

The bathymetry of the South China Sea has been studied by Wang et al. (2001) using satellite derived gravity data and a spectral approach to the isostatic flexure. The short wavelength bathymetry in the band 20-120 km is recovered from gravity by downward continuation, and the long wavelength part is set equal to the ETOPO5 grid. It was shown that the inversion recovered several tectonic features not present in the ETOPO5 model.

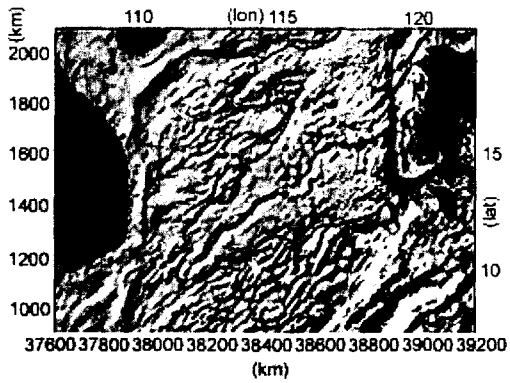

Fig. 2 Observed satellite derived gravity anomaly (Hwang et al., 1998). Land areas: black.

4 The China Sea CMI and Bathymetry

The above method is applied to the South China Sea, in an area defined in latitude by the interval 8°N-19°N and in longitude by 105°E-122°E. The window comprises the central part of the South China Sea basin. The observed gravity anomaly is shown in Fig. 2, and the land (dry) areas are marked in black. The satellite derived gravity field with 2' x 2' sampling of Hwang et al. (1998) was projected in Gauss Krueger projection and resampled at 4 km grid interval. The most evident feature is given by the negative gravity values along the rift. Isolated bright spots are due to seamounts or small features emerging above the basin. The Nansha Trough and the Manila Trench are marked by strongly negative gravity values. The complete Bouguer correction was applied with a density of 1.64 10^3 kg/m^3. Here the ETOPO5 model was used for the calculations. The Bouguer field is low pass filtered with a cosine taper filter which has unit value to a wavelength of

120km. This field is used for the constrained inversion of the CMI (Step A1). The constraining values of the depth of the CMI are taken from Xu et al., (1997), and refer to seismic investigations.

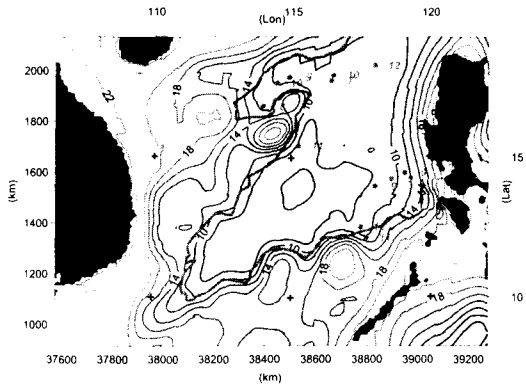

Fig. 3 Solution of the CMI undulations in South China Sea from gravity inversion and flexural modeling. Land areas: black. Seismic constraints on CMI depth after Xu et al. (1997) as labeled grey dots. Isoline spacing: 2km. Outline of basin: grey.

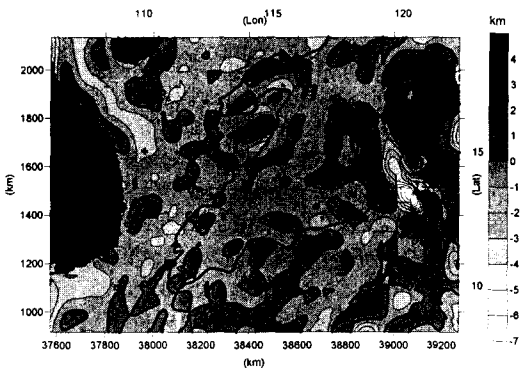

Fig. 4 Difference between CMI undulations from gravity inversion and according to flexure model (km). Land areas: black. Outline of basin black.

In Fig. 3 the position and values of the constraints on the CMI are plotted as labeled dots. Different values of the reference depth d of the CMI, ranging from 20-30 km, and of the density contrast (450-570 kg/m^3) were tested. Smallest mean deviations from the constraining values are found for d=21-23 km and density between 470 and 550 kg/m^3, the greater reference depth requiring a smaller density contrast.

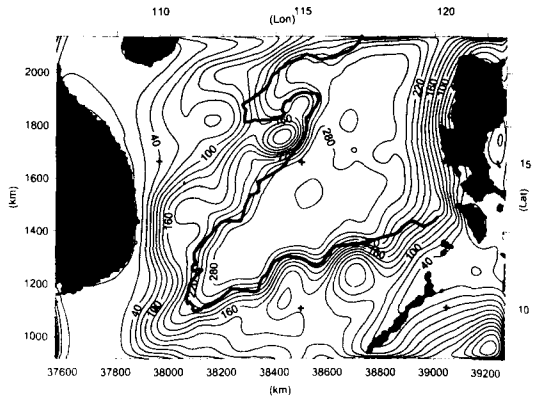

Fig. 5 Gravity field of the CMI, isolines spacing: 20 10^{-5} m/s^2. Outline of basin: heavy black. Land areas: black.

We now test the compatibility of this field with the isostatic flexure model, where the elastic thickness is allowed to vary spatially (Step A2). On square windows of 120 km sides the T_e values are found for which the gravity inverted CMI and the flexure CMI variations have the smallest rms-difference. The windows are shifted by 50% of their sidelengths. The solution of the CMI undulations according to the flexure model are shown in Fig. 3. The flexure CMI reproduces the gravity CMI very well in the basin. The difference (gravity CMI - flexure CMI) is shown in Fig. 4. The overall difference ranges in the bounds -7 to +4 km, the greatest values being found east of the Manila Trench. The standard deviation is 1 km. The flexure CMI represents a physical model of the crustal thickness variations in the frame of the thin-plate isostatic flexure model. We thus calculated the corresponding gravity field (Step B), shown in Fig. 5. This field is subtracted from the observed field, furnishing the residual field. The residual field is then inverted in order to recover the bathymetry (Step C). The reference depth d is set at the surface and the density contrast is adjusted so as to minimize the difference between the inverted bathymetry and the shiptrack derived bathymetry. We let the density vary in the bounds 1450 to 1650 kg/m^3, and assign the value 1640 kg/m^3, which leads to a good fit to the constraining bathymetric values. The final bathymetry grid for the South China Sea is shown in Fig. 6. The inverted bathymetry and the starting values of ETOPO5 on average differ by an amount of 230m (root mean square), with extremes reaching isolated maximum values of ± 2000 m. Along the SW part of the rift, present as a linear feature in the gravity anomaly, a deepening of the bathymetry is found, of about 500 m. The rift structure is hardly

present in the shiptrack data, which is an indication of the fact that it must be buried below sediments.

Along the profiles A-D marked in Fig. 6, a comparison between the different fields is made. The flexure and gravity CMI, the different bathymetry estimations (ETOPO5, inversion of this paper, bathymetry of Sandwell and Smith (1997), shiptracks) and the gravity field (observed gravity anomaly, Bouguer gravity, and gravity field of the flexure CMI) are shown in Fig. 7. It is seen that the flexure and gravity CMI are in good agreement, and that the long-wavelength part of the Bouguer gravity coincides with the gravity field of the flexure CMI. With respect to the ETOPO5 grid, the bathymetry estimate from the inversion contains more detail.

The deepening of the bathymetry along the rift is more pronounced in the SW, younger part of the basin (profiles C, D), whereas in the NE part it is lined by a series of seamounts. The profiles show well how the deepening of the basin is accompanied by a shallowing of the CMI, giving evidence of isostatic equilibrium. The elastic thickness we find in the basin is generally low and varies between 2 and 6 km.

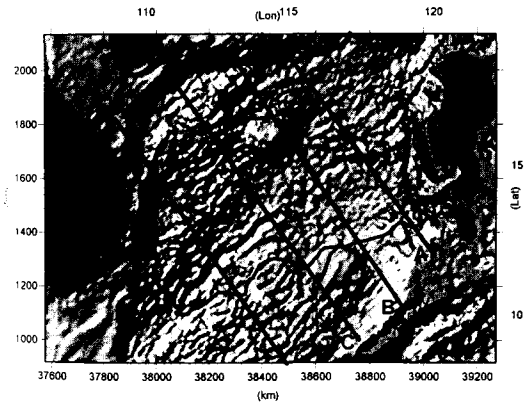

Fig. 6 Bathymetry grid from gravity inversion. Profiles A,B,C,D shown in Fig. 7. Land areas: black. Basin outline: heavy black.

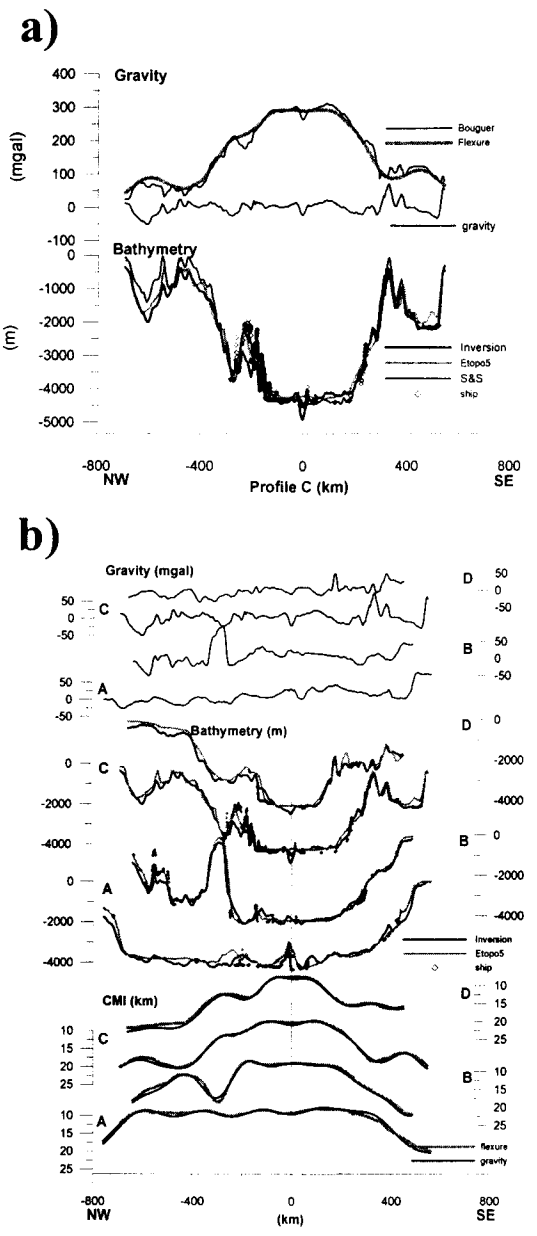

Fig. 7 The different quantities along the profiles shown in Fig. 6 (origin centered on the intersection with the rift). a) profile C: bathymetry according to this paper, to ETOPO5, to Sandwell and Smith (1997), to shiptracks and gravity field (observed anomaly, Bouguer, gravity field of flexure CMI) b) profiles A-D: flexure and gravity CMI, bathymetry (inversion, ETOPO5, shiptracks) and gravity anomaly.

5 Discussion and Conclusion

We have described a method that aims at formulating a model of the crustal thickness variations and of the

bathymetry, using the satellite derived global gravity grid and the thin plate lithospheric flexure model. The solution is constrained by available data regarding crustal thickness and bathymetry, available along profiles, or at single points. The method we propose takes most of the gravity signal into account, and limitations are made only for the very long wavelengths (>800 km). The observed gravity field is modelled as the sum of the contribution of the CMI undulations and of the bathymetry. Intracrustal mass-anomalies are not presently taken into account, as no sufficient information is presently available to us. The methodology can be extended in its application to a large scale study of the CMI-undulations and bathymetry. Ideally the effects of sediments on the gravity field should be modelled. As we had no constraints on the sediment cover, this could not be done in the South China Sea at the present time, but is a goal for the future. The neglect of the sediment cover can lead to an overestimation of the crustal thickness, in places where the sediment cover effectively is present.

The presence of the sediment cover opens another problem, of more fundamental nature. As discussed in Smith and Sandwell (1997), features of the basaltic oceanic crust, closely tied to the teconic evolution of the sea-floor, can be partly or completely masked by a loose sedimentary cover.

Depending on the specific application for which the bathymetry grid is used, the undulations of the oceanic basaltic crust may be preferred to the bathymetric model corresponding to the surface formed by the sediments.

Due to the strong gravity signal produced by the undulations of the basaltic oceanic crust, the bathymetry obtained from the inversion of the observed gravity anomaly, is nearly coincident with this last surface. It follows that important features of the bathymetry are recovered from the gravity inversion, that may not be visible by shipsounding due to the fact that they are buried below sediments.

An example is the rift structure in the South China Sea, which is missing in the ETOPO5 model, but is clearly visible in the inverted bathymetry. For all applications that are concerned with the study of the geological/geophysical properties of the ocean floor, the gravity inverted bathymetry is of great use and may be preferred to the ship-borne bathymetry. On the contrary, for all applications that concern navigation and mapping of the present seafloor, the bathymetry which equivals to the depth recoverable by shipsounding is the one to be used.

Acknowledgement. We acknowledge support from the Italian CNR and Chinese CAS, in particular in the frame of the Italian-Chinese exchange program and from the University of Trieste and Italian MIUR. We thank for the use of the GMT- software package (Wessel and Smith, 1998).

References

Blakely, R. J. (1995). Potential Theory in Gravity and Magnetic Applications, Cambridge University Press, Cambridge, pp. 1-441.

Braitenberg, C., F. Pettenati and M. Zadro (1997). Spectral and Classical Methods in the Evaluation of Moho Undulations from Gravity Data: the NE Italian Alps and Isostasy, J Geodyn, 23, pp. 5-22.

Braitenberg, C., and R. Drigo (1997). A Crustal Model from Gravity Inversion in Karakorum, in: Int. Symp. on Current Crustal Movement and Hazard Reduction in East Asia and South-East Asia, Wuhan, November 4-7, 1997, Symposia Proceeding, pp. 325-341.

Braitenberg, C., and M. Zadro (1999). Iterative 3D Gravity Inversion with Integration of Seismologic Data, Bollettino di Geofisica Teorica ed Applicata, 40, pp. 469-476.

Braitenberg, C., J. Ebbing and H. J. Götze (2002). Inverse Modelling of Elastic Thickness by Convolution Method - the Eastern Alps as a Case Example, Earth Planet Sci Lett, 202, pp. 387-404.

Ebbing, J., C. Braitenberg and H. J. Götze (2001). Forward and Inverse Modelling of Gravity Revealing Insight into Crustal Structures of the Eastern Alps, Tectonophysics, 337, pp. 191-208.

Hwang, C., E. C. Kao and B. Parsons (1998). Global Derivation of Marine Gravity Anomalies from Seaset, Geosat, ERS-1 and TOPEX/POSEIDON Altimeter Data, Geophys J Int, 134, pp. 449-459.

Map Series of Geology and Geophysics of China Sea and Adjacent Regions (1992). Ministry of Geology and Mineral Resources, P.R. China, Geological Publishing House, P.R. China.

Nissen, S. S., D. E. Hayes, B. Yao, W. Zeng, Y. Chen and X. Nu (1995). Gravity, Heat Flow, and Seismic Constraints on the Processes of Crustal Extension: Northern Margin of the South China Sea, J Geophys Res, 100, pp. 22447-22483.

Sandwell, D. T., and W. H. F. Smith (2001). Bathymetric Estimation, in: Satellite Altimetry and Earth Sciences, Eds. Fu L-L and Cazenave A, Academic Press, pp. 441-457.

Smith, W. H. F., and D. T. Sandwell (1997). Global Sea Floor Topography from Satellite Altimetry and Ship Depth Soundings. Science, 277, pp. 1956-1962.

Wang, Y., H. Xu and J. Zhan (2001). High Resolution Bathymetry of China Seas and Their Surroundings, Chinese Science Bulletin, 46, pp. 1661-1664.

Watts, A. B. (2001) Isostasy and Flexure of the Lithosphere, Cambridge University Press, Cambridge, 2001, pp. 458.

Wessel, P., and W. H. F. Smith (1998). New, Improved Version of the Generic Mapping Tools released, EOS Trans AGU, 79, pp. 579.

Xu, D., X. Liu, X. Zhang, et al (1997). China Offshore Geology, Geological Publishing House Bejing, pp. 247-252.

Zadro, M. (1986). Spectral Images of the Gravitational Field. Manuscript Geodetic, 11, pp. 207-213.

Zadro, M., and C. Braitenberg (1997). Spectral Methods in Gravity Inversion: the Geopotential Field and its Derivatives. Annali di Geofisica XL (5), pp. 1433-1443.